# Soil creep in salt marshes

**G. Mariotti[1], W.S. Kearney[2], and S. Fagherazzi[2]**

*[1]Louisiana State University, Department of Oceanography and Coastal Sciences, Center for Computation and Technology, Baton Rouge, Louisiana 70803, USA*

*[2]Boston University, Department of Earth and Environment, Boston, Massachusetts 02118, USA*

**DATA REPOSITORY**

## 1. Summary of vertical accretion rates from various salt marshes wordwide

Table DR1: Net sediment accumulation of sediment (expressed in mm/yr) measured at different distances from the channel edge. Channel-side locations include area 0 to 5 m from the channel edge, marsh interior includes areas at least 30 m from the channel edge.

| Source | Geographic location | Channel -side | Interior | Relative sea level rise rate |
|---|---|---|---|---|
| (Letzsch and Frey, 1980) | Sapelo Sound, GA (USA) | 12 | 1 | 1-2 |
| (Stock, 2011) | Schleswig-Holstein (Germany) | 17 | 5 | 4.2 |
| (Suchrow et al., 2012) | North Sea (Germany) | 12 | 2 | 1-2 |
| (Chmura et al., 2001) | Bay of Fundy (Canada) | 10-50 | 2 | Not reported |
| (Esselink et al., 1998) | Dollard Estuary (Netherlands) | 15-16 | 0-2 | Not reported |
| (French and Spencer, 1993); (Stoddart et al., 1989) | Scolt Head Island, Norfolk (UK) | 8 | 2 | 2 |
| (Craft et al., 1993) | Outer Banks, NC (USA) | 2.8-3.7 | 0.9-2.3 | 1.9 |
| (Butzeck et al., 2014) | Elbe Estuary (Germany) | 5.8-20.3 | 1.1-3.1 | 3.6 |
| (Oenema and DeLaune, 1988) | Eastern Scheldt (Netherlands) | 16 | 10.1 | 4 |
| (Reed, 1988) | Dengie Peninsula, Essex (UK) | 10-20 | 5-10 | 3 |
| (Carling, 1982) | Burry Inlet, South Wales (UK) | 50 | 10-20 | |
| (Donnelly and Bertness, 2001) | Narragansett Bay, RI (USA) | 4.9 | 2 | 2.7 |
| (Kearney et al., 1994) | Chesapeake Bay, MD (USA) | 2-5 | 2-3.5 | |
| (Bricker-Urso et al., 1989) | Narragansett Bay, RI (USA). | 4.3 | 2.4 | 2.6 |
| **Mean and standard deviation** | | 14.1 ±13.0 | 4.0 ±4.1 | 2.7 ±1.0 |

## 2. Calculation of channel widths


Figure DR1. Map of the study site in Plum Island Sound (MA). Googlearth image (aquired on 6/6/2015).

Channel widths were calculated in both the reference and the nutrient enriched channels (Fig. 1) using the aerial images. In each channel, thirty widths were measured as the distance at the base of the banks (the inner boundary).

Table DR2. Channel widths measured in the nutrient enriched and in the reference channel. Errors are reported as one standard deviations.

| | **Enriched 2010** | **Enriched 2014** | **Reference 2010** | **Reference 2014** |
|---|---|---|---|---|
| **Width** | 3.5±1.1 | 3.4±1.2 | 4.0±2.2 | 3.7±2.1 |
| **Width difference (2014 - 2010)** | -0.1±0.82 | | -0.3±0.7 | |

## 3. Auxiliary data from Plum Island

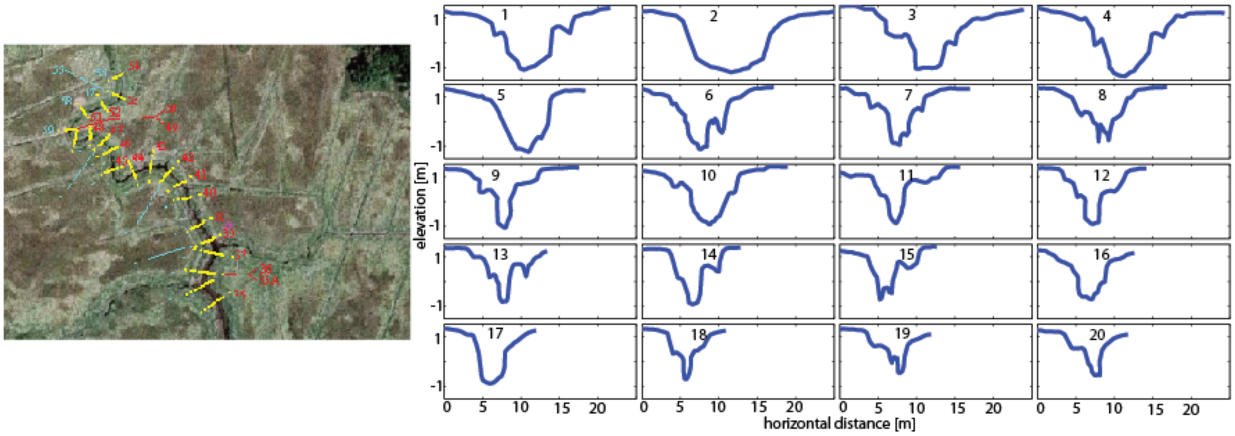


Figure DR2. Cross sections of the reference creek (see Fig. 1). Note the absence of levees and the presence of concave thalwegs and convex banks. Cross section numbers increase upstream.

Figure DR3. Image of the slumping banks in the reference creek. Note the convexity of the upper banks, suggesting the presence of a soil diffusion process.

## 4. Details of the model

The bed elevation along the transect, *h*, is discretized with a spatial resolution of 0.2 m, which allows to reproduce the geometry of the banks in details.

The yearly-peak vegetation biomass, *B*, is calculated at each point in the transect as

$$B = \begin{cases} 0 & H < H_{\min} \\ B_m \dfrac{\left(H - H_{\min}\right)\left(H_{\max} - H\right)}{\left(H_{\max} - 3H_{\min}\right)\left(H_{\max} + H_{\min}\right)/4} & H_{\min} < H < H_{\max} \\ 0 & H > H_{\max} \end{cases} \qquad \text{(S1)}$$

where *H* is the depth with respect to the high tide level, $B_m$ is the peak aboveground biomass reached at the optimum elevation, $H_{min}$ and $H_{max}$ are the minimum and maximum depths that allows vegetation growth, which for simplicity are set equal to 0 and 0.737*r* - 0.092 (McKee and Patrick, 1988), where *r* is the tidal range. The organogenic sedimentation is calculated as $O{=}T_G \mu_G \chi_r B$, where $T_G$ is the growth period, set equal to half a year, $\mu_G$ is the growth rate, and $\chi_r$ is the refractory fraction.

The erosional and depositional terms are computed using a simplified model for tidal flow. Assuming that the slope of the water surface is smaller across the channel than along the channel (Mariotti and Fagherazzi, 2012), a uniform water level is imposed over the cross section at each time step. The time variable water level, *y*, is described by a sinusoidal curve with a period *T* and an amplitude *r*/2. In order to recreate a more realistic flow during the wetting and drying phase, a modification of the bed elevation and the fraction of the wetted area, *η*, is introduced (Defina, 2000). Assuming that the bed elevation irregularities are distributed normally with a standard deviation equal to *k*/2, the fraction of wetted area is computed as $\eta = 0.5\left\{1 = erf\left[\left(y-h\right)/k\right]\right\}$, and the effective the water depth, *d*, is calculated as $d = \eta\left(y-h\right) + \exp\left\{-4\left[\left(y-h\right)/k\right]^2\right\}/\left(4\sqrt{\pi}\right)$ (Defina, 2000). Assuming a quasi-static propagation of the water level (Fagherazzi et al., 2003) the instantaneous discharge through the cross section, *Q*, is computed as

$$Q = \int_0^W \eta U_\xi d\mathrm{d}x = \int_0^W q_\xi \mathrm{d}x = L\int_0^W \eta \frac{\mathrm{d}y}{\mathrm{d}t}\mathrm{d}x \quad (S2)$$

where $q_\xi$ is the along-channel discharge per unit of width and $U_\xi$ is the along-channel velocity. The along-channel velocity is computed at each point of the transect by redistributing the instantaneous discharge to satisfy the frictional balance (Mariotti and Fagherazzi, 2013), $U_\xi \propto \sqrt{d/C}$, where the total drag coefficient $C$ is the sum of a constant bed drag, $C_b$, and a stem drag, $C_v$. Assuming that the vegetation is always emergent, the stem drag is computed as $C_v=1/2a_sd$, where $a_s$ is the projected stem area, calculated as $0.25B^{0.5}$ (Mudd et al., 2004), and where the drag coefficient for an individual stem is assumed equal to 1 (Baptist et al., 2007). The cross-channel discharge per unit of width, $q_x$, is then computed by imposing the conservation of water mass flowing through the transect (Mariotti and Fagherazzi, 2012),

$$q_x = \int_0^W \left( L\eta \frac{\mathrm{d}y}{\mathrm{d}y} - \frac{\mathrm{d}q_\xi}{\mathrm{d}\xi} \right) \mathrm{d}x \quad (S3)$$

The erosion term is computed as $E = \max\left[0, m_e\left(\tau - \tau_{cr}\right)/\tau_{cr}\right]$ (Whitehouse et al., 2000), where the erodability coefficient, $m_e$, and the critical bed shear stress, $\tau_{cr}$, are fixed parameters, and the bed shear stress $\tau$ is computed as a function of the along channel velocity. The bed shear stress is computed using only the bed drag, $\tau = \rho_w C_b U_\xi^2$, where $\rho_w$ is the water density. Because of the quasi-steady assumption and the small depth-to-tidal-range ratio, the bed shear stresses in the channel can achieve unrealistic large values when the water level is close to mean sea level. In order to reproduce the occurrence of a velocity surge only during the wetting and drying of the platform (French and Stoddart, 1992; Fagherazzi et al., 2008), the bed shear stress is set equal to zero when the water level is below the lowest point of the marsh platform.

The deposition term $D$ is calculated as the product of the effective settling velocity $w_s$ and the suspended sediment concentration near the bed, which is set equal to twice the depth average concentration $c$. The effective settling velocity is the sum of a constant value $w_{s,o}$, and a vegetation induced sedimentation, $w_{s,v}$. The suspended sediment concentration is highly variable in space and time, and it is computed with the following mass balance,

$$\frac{\partial(dc)}{\partial t} = -D + E + \frac{\partial\left(c_i q_\xi\right)}{\partial \xi} - \frac{\partial\left(c q_x\right)}{\partial x} + \frac{\partial\left(\upsilon_s d\left(\partial c/\partial x\right)\right)}{\partial x} \quad (S4)$$

where the first two terms on the right hand side are the sink and source as in Eq. 1, the third term is the along-channel advection, the fourth term is the cross-channel advection and the fifth term is the cross-channel diffusion, where $v_s$ is the horizontal eddy diffusivity coefficient. The horizontal eddy diffusivity is set equal to $0.13du_*$ (Fischer, 1973), where for simplicity the friction velocity is set uniform and it is computed using a constant bed shear stress equal to the critical value, $u_* = \sqrt{\tau_{cr} / \rho_w}$ . Eq. S4 is analogous to that used by Marani et al. (2013), except that it includes sediment resuspension and along channel transport. The latter is accounted for by using a simplified approach (Krone, 1962; Temmerman et al., 2004): during the ebb phase the concentration is set constant along the channel direction, that is $c_i = c$; during flood the along channel advection term is computed imposing a boundary concentration, that is $c_i = c_o$. As a result the sediment concentration in the cross section stems from a combination of the sediment boundary condition $c_o$ and by local dynamics in the channel, whereas previous models assumed that the suspended sediment concentration in the channel is imposed a priori (D'Alpaos et al., 2006; Kirwan and Guntenspergen, 2010). It is important to note that if $c_i$ is set equal to zero during both ebb and flood then the sum of the inorganic sediment in the bed and in suspension is instantaneously conserved; whereas if $c_i$ is set equal to $c$ during both ebb and flood and if a dynamic equilibrium is reached, then the sum of the inorganic sediment is conserved over a tidal cycle.

All equations are solved simultaneously with an implicit finite-volume method, using a time step of 5 minute.

Table DR3. Reference parameters used in the model.

| Name | Description | Value | Reference | Name | Description | Value | Reference |
|---|---|---|---|---|---|---|---|
| $c_o$ | Boundary suspended sediment concentration | 10 mg/l | | $B_m$ | Maximum aboveground yearly-peak biomass | 2.5 kg/m$^2$ | (Mudd et al., 2009; Morris et al., 2013) |
| $m_e$ | Erodibility parameter | 0.001 kg/m$^2$/s | Whitehouse et al. (2000) | $K_{mud}$ | Unvegetated soil diffusivity | 2 m$^2$/yr | (Kirwan and Murray, 2007) |
| $\tau_{cr}$ | Critical shear stress for erosion | 0.1 Pa | Whitehouse et al. (2000) | $K_{veg}$ | Vegetated soil diffusivity | 0.3 m$^2$/yr | Calibrated |
| $W$ | Platform width | 75 m | | $R$ | Sea level rise rate | 2.6 mm/yr | Wilson et al. (2014) |
| $w_{s,o}$ | Settling velocity | 0.2 mm/s | Whitehouse et al. (2000) | $C_b$ | Bed drag coefficient | 0.005 | Nepf (1999) |
| $\rho_w$ | Water density | 1030 kg/m$^3$ | | $T$ | Tidal period | 12.5 h | |
| $\rho_s$ | Inorganic sediment dry bulk density | 1000 kg/m$^3$ | | $r$ | Mean tidal range | 2.7 m | NOAA Station: 844 1241 |
| $\rho_o$ | Organic sediment dry bulk density | 120 kg/m$^3$ | | $k$ | Bed elevation variability | 0.5 m | |
| $H_{min}$ | Min inundation depth | 0 | (McKee and Patrick, 1988) | $\mu_G$ | Plant growth rate | 0.0138 1/day | (Mudd et al., 2009) |
| $H_{max}$ | Max inundation depth | 0.737$r$-0.092 = 1.9 m | (McKee and Patrick, 1988) | $\chi_{ref}$ | Refractory organic matter fraction | 0.158 | (Mudd et al., 2009) |

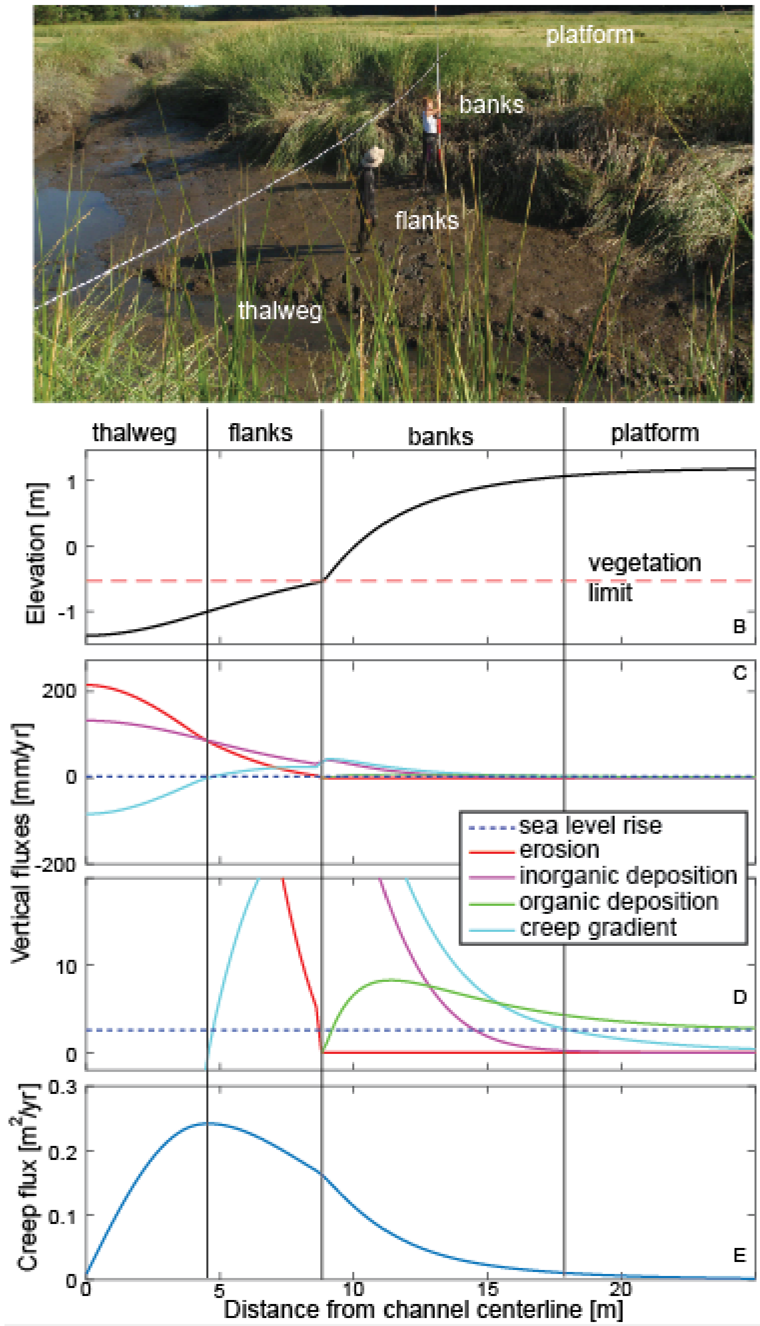


Figure DR4. Predicted cross sections and sediment fluxes at steady state in a scenario where channel flanks are present ($L$ = 1000 m, $K_{veg}$ = 0.3 m$^2$/yr, $c_o$ = *10* mg/l, same as figure 2). A) Picture of a channel with flanks. B) Dynamic equilibrium predicted by the model. C,D) Vertical fluxes as in Eq. 1, plotted with two different vertical scales. Note that on the flanks, as on the banks, the creep gradient is positive E) Creep flux.

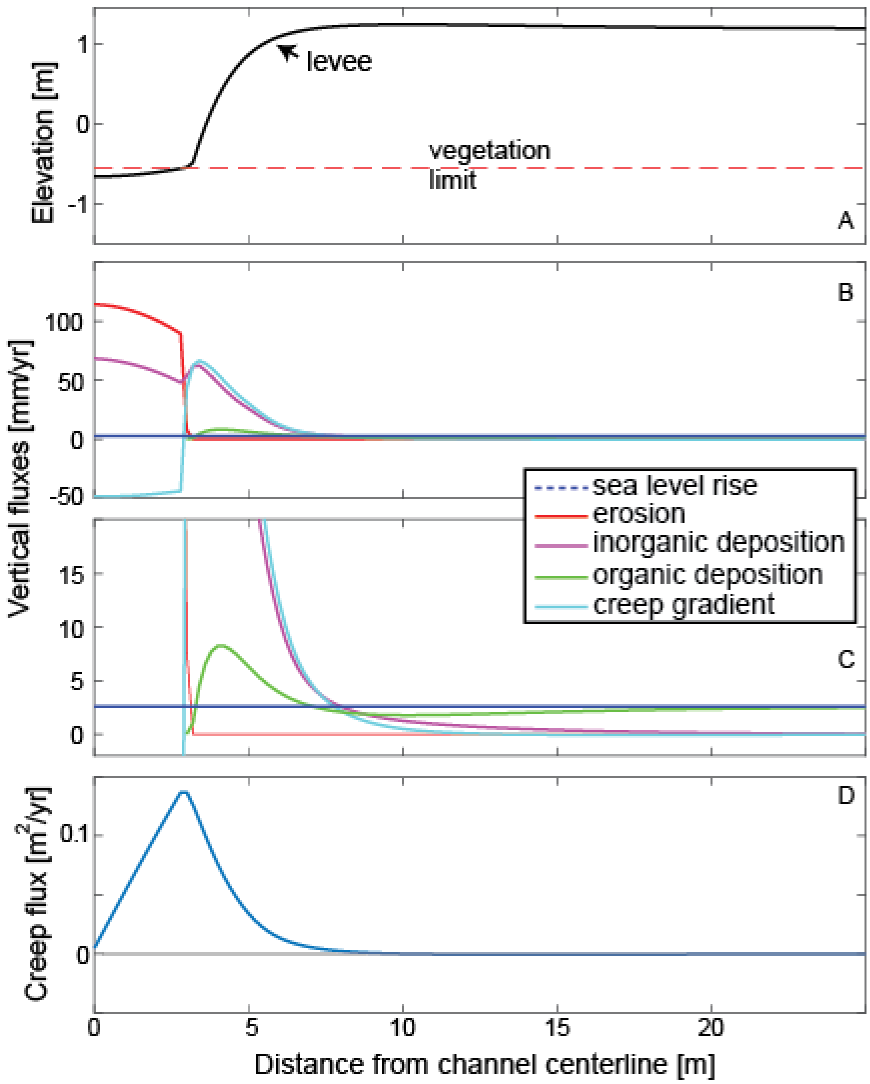


Figure DR5. Predicted cross sections and sediment fluxes at steady state in a scenario where a levee is present ($L$ = 400 m, $c_o$ = *10* mg/l, $K_{veg}$ = 0.1 m$^2$/yr, same as figure 4). A) Dynamic equilibrium predicted by the model. B,C) Vertical fluxes as in Eq. 1, plotted with two different vertical scales. D) Creep flux. Note that for $x$ > 10 m the creep flux is negative (toward the marsh interior), but is negligible compared to the positive flux (toward the channel) that is present for $x$ < 10 m.

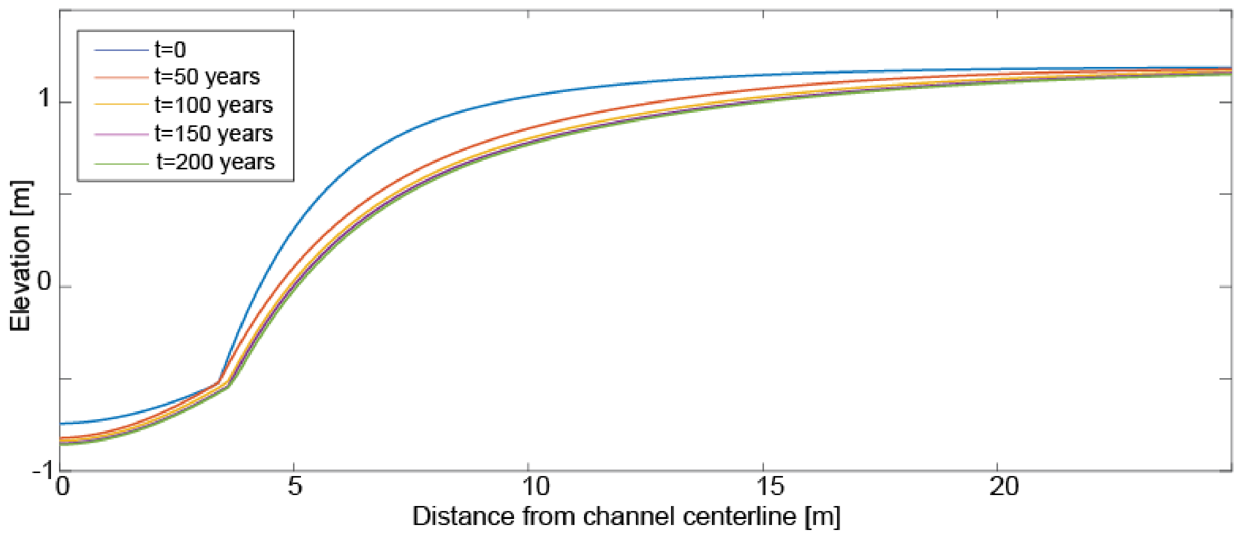


Figure DR6. Transient evolution of the cross section after a doubling in soil diffusivity ($K_{veg}$ from 0.3 to 0.6 $m^2/yr$). The new equilibrium is reached after about 100 years. Even though the channel deepens and the bank becomes less steep, the position of the base of the bank changes by only 0.2 m after the new dynamic equilibrium is reached.

## References

Baptist, M.J., Babovic, V., Uthurburu, J.R., Keijzer, M., Uittenbogaard, R.E., Mynett, A., and Verwey, A., 2007, On inducing equations for vegetation resistance: Journal of Hydraulic Research, v. 45, no. 4, p. 435–450, doi: 10.1080/00221686.2007.9521778.

Bricker-Urso, S., Nixon, S.W., Cochran, J.K., Hirschberg, D.J., and Hunt, C., 1989, Accretion rates and sediment accumulation in Rhode Island salt marshes: Estuaries, v. 12, no. 4, p. 300–317, doi: 10.2307/1351908.

Butzeck, C., Eschenbach, A., Gröngröft, A., Hansen, K., Nolte, S., and Jensen, K., 2014, Sediment Deposition and Accretion Rates in Tidal Marshes Are Highly Variable Along Estuarine Salinity and Flooding Gradients: Estuaries and Coasts, v. 38, no. 2, p. 434–450, doi: 10.1007/s12237-014-9848-8.

Carling, P.A., 1982, Temporal and spatial variation in intertidal sedimentation rates: Sedimentology, v. 29, no. 1, p. 17–23, doi: 10.1111/j.1365-3091.1982.tb01705.x.

Chmura, G.L., Coffey, A., and Crago, R., 2001, Variation in Surface Sediment Deposition on Salt Marshes in the Bay of Fundy: Journal of Coastal Research, v. 17, no. 1, p. 221–227.

Craft, C.B., Seneca, E.D., and Broome, S.W., 1993, Vertical Accretion in Microtidal Regularly and Irregularly Flooded Estuarine Marshes: Estuarine, Coastal and Shelf Science, v. 37, no. 4, p. 371–386, doi: 10.1006/ecss.1993.1062.

D’Alpaos, A., Lanzoni, S., Mudd, S.M., and Fagherazzi, S., 2006, Modeling the influence of hydroperiod and vegetation on the cross-sectional formation of tidal channels: Estuarine Coastal and Shelf Science, v. 69, p. 311–324, doi: 10.1016/j.ecss.2006.05.002.

Defina, A., 2000, Two-dimensional shallow flow equations for partially dry areas: Water Resources Research, v. 36, p. 3251–3264.

Donnelly, J.P., and Bertness, M.D., 2001, Rapid shoreward encroachment of salt marsh cordgrass in response to accelerated sea-level rise: Proceedings of the National Academy of Sciences, v. 98, no. 25, p. 14218–14223, doi: 10.1073/pnas.251209298.

Esselink, P., Dijkema, K.S., Reents, S., and Hageman, G., 1998, Vertical Accretion and Profile Changes in Abandoned Man-Made Tidal Marshes in the Dollard Estuary, the Netherlands: Journal of Coastal Research, v. 14, no. 2, p. 570–582.

Fagherazzi, S., Hannion, M., and D’Odorico, P., 2008, Geomorphic structure of tidal hydrodynamics in salt marsh creeks: Water Resources Research, v. 44, p. 12, doi: 10.1029/2007wr006289.

Fagherazzi, S., Wiberg, P.L., and Howard, A.D., 2003, Tidal flow field in a small basin: Journal of Geophysical Research: Oceans, v. 108, no. C3, p. 3071, doi: 10.1029/2002JC001340.

Fischer, H.B., 1973, Longitudinal Dispersion and Turbulent Mixing in Open-Channel Flow: Annual Review of Fluid Mechanics, v. 5, no. 1, p. 59–78, doi: 10.1146/annurev.fl.05.010173.000423.

French, J.R., and Spencer, T., 1993, Dynamics of sedimentation in a tide-dominated backbarrier salt marsh, Norfolk, UK: Marine Geology, v. 110, no. 3–4, p. 315–331, doi: 10.1016/0025-3227(93)90091-9.

French, J.R., and Stoddart, D.R., 1992, Hydrodynamics of salt marsh creek systems: Implications for marsh morphological development and material exchange: Earth Surface Processes and Landforms, v. 17, no. 3, p. 235–252, doi: 10.1002/esp.3290170304.

Kearney, M.S., Stevenson, J.C., and Ward, L.G., 1994, Spatial and temporal changes in marsh vertical accretion rates at Monie Bay: Implications for sea-level rise: Journal of Coastal Research, v. 10, no. 4, p. 1010–1020.

Kirwan, M.L., and Guntenspergen, G.R., 2010, Influence of tidal range on the stability of coastal marshland: Journal of Geophysical Research: Earth Surface, v. 115, no. F2, p. n/a–n/a, doi: 10.1029/2009JF001400.

Kirwan, M.L., and Murray, A.B., 2007, A coupled geomorphic and ecological model of tidal marsh evolution: Proceedings of the National Academy of Sciences, v. 104, no. 15, p. 6118–6122, doi: 10.1073/pnas.0700958104.

Krone, R.B., 1962, Flume studies of the transport of sediment in estuarial shoaling processes;final report,: Berkeley :

Letzsch, W.S., and Frey, R.W., 1980, Deposition and erosion in a Holocene salt marsh, Sapelo Island, Georgia: Journal of Sedimentary Research, v. 50, no. 2, p. 529–542, doi: 10.1306/212F7A45-2B24-11D7-8648000102C1865D.

Marani, M., Lio, C.D., and D'Alpaos, A., 2013, Vegetation engineers marsh morphology through multiple competing stable states: Proceedings of the National Academy of Sciences, p. 201218327, doi: 10.1073/pnas.1218327110.

Mariotti, G., and Fagherazzi, S., 2013, A two-point dynamic model for the coupled evolution of channels and tidal flats: Journal of Geophysical Research: Earth Surface, p. n/a–n/a, doi: 10.1002/jgrf.20070.

Mariotti, G., and Fagherazzi, S., 2012, Channels-tidal flat sediment exchange: The channel spillover mechanism: Journal of Geophysical Research: Oceans, v. 117, no. C3, p. n/a–n/a, doi: 10.1029/2011JC007378.

McKee, K.L., and Patrick, W.H., Jr., 1988, The relationship of smooth cordgrass (Spartina Alterniflora) to tidal datums: A review: Estuaries, v. 11, no. 3, p. 143–151, doi: 10.2307/1351966.

Morris, J., Sundberg, K., and Hopkinson, C., 2013, Salt marsh primary production and its responses to relative sea level and nutrients in estuaries at Plum Island, Massachusetts, and North Inlet, South Carolina, USA.: Oceanography, v. 26, p. 78–84.

Mudd, S.M., Fagherazzi, S., Morris, J.T., and Furbish, D.J., 2004, Flow, Sedimentation, and Biomass Production on a Vegetated Salt Marsh in South Carolina: Toward a Predictive Model of Marsh Morphologic and Ecologic Evolution, *in* Fagherazzi, S., Marani, M., and Blum, L.K. eds., Coastal and Estuarine Studies, American Geophysical Union, Washington, D. C., p. 165–188.

Mudd, S.M., Howell, S.M., and Morris, J.T., 2009, Impact of dynamic feedbacks between sedimentation, sea-level rise, and biomass production on near-surface marsh stratigraphy and carbon accumulation: Estuarine, Coastal and Shelf Science, v. 82, no. 3, p. 377–389, doi: 10.1016/j.ecss.2009.01.028.

Oenema, O., and DeLaune, R.D., 1988, Accretion rates in salt marshes in the Eastern Scheldt, South-west Netherlands: Estuarine, Coastal and Shelf Science, v. 26, no. 4, p. 379–394, doi: 10.1016/0272-7714(88)90019-4.

Reed, D.J., 1988, Sediment dynamics and deposition in a retreating coastal salt marsh: Estuarine, Coastal and Shelf Science, v. 26, no. 1, p. 67–79, doi: 10.1016/0272-7714(88)90012-1.

Stock, M., 2011, Patterns in surface elevation change across a temperate salt marsh platform in relation to sea-level rise: Coastline Reports, v. 17.3.

Stoddart, D.R., Reed, D.J., and French, J.R., 1989, Understanding Salt-Marsh Accretion, Scolt Head Island, Norfolk, England: Estuaries, v. 12, no. 4, p. 228–236, doi: 10.2307/1351902.

Suchrow, S., Pohlmann, N., Stock, M., and Jensen, K., 2012, Long-term surface elevation changes in German North Sea salt marshes: Estuarine, Coastal and Shelf Science, v. 98, p. 71–83, doi: 10.1016/j.ecss.2011.11.031.

Temmerman, S., Govers, G., Meire, P., and Wartel, S., 2004, Simulating the long-term development of levee–basin topography on tidal marshes: Geomorphology, v. 63, no. 1–2, p. 39–55, doi: 10.1016/j.geomorph.2004.03.004.

Whitehouse, R., Soulsby, R., Roberts, W., and Mitchener, H., 2000, Dynamics of estuarine muds: Thomas Telford Publishing.